Video Article

Atomic Force Microscopy of Red-Light Photoreceptors Using PeakForce Quantitative Nanomechanical Property Mapping

Marie E. Kroeger[1], Blaire A. Sorenson[2], J. Santoro Thomas[2], Emina A. Stojković[1], Stefan Tsonchev[2], Kenneth T. Nicholson[2]

[1]Department of Biology, Northeastern Illinois University

[2]Department of Chemistry, Northeastern Illinois University

Correspondence to: Kenneth T. Nicholson at k-nicholson@neiu.edu

URL: https://www.jove.com/video/52164
DOI: doi:10.3791/52164

Keywords: Physics, Issue 92, atomic force microscopy, protein, photoreceptor, surface chemistry, nanoscience, soft materials, macromolecules, AFM

Date Published: 10/24/2014

Citation: Kroeger, M.E., Sorenson, B.A., Thomas, J.S., Stojković, E.A., Tsonchev, S., Nicholson, K.T. Atomic Force Microscopy of Red-Light Photoreceptors Using PeakForce Quantitative Nanomechanical Property Mapping. *J. Vis. Exp.* (92), e52164, doi:10.3791/52164 (2014).

Abstract

Atomic force microscopy (AFM) uses a pyramidal tip attached to a cantilever to probe the force response of a surface. The deflections of the tip can be measured to ~10 pN by a laser and sectored detector, which can be converted to image topography. Amplitude modulation or “tapping mode” AFM involves the probe making intermittent contact with the surface while oscillating at its resonant frequency to produce an image. Used in conjunction with a fluid cell, tapping-mode AFM enables the imaging of biological macromolecules such as proteins in physiologically relevant conditions. Tapping-mode AFM requires manual tuning of the probe and frequent adjustments of a multitude of scanning parameters which can be challenging for inexperienced users. To obtain high-quality images, these adjustments are the most time consuming.

PeakForce Quantitative Nanomechanical Property Mapping (PF-QNM) produces an image by measuring a force response curve for every point of contact with the sample. With ScanAsyst software, PF-QNM can be automated. This software adjusts the set-point, drive frequency, scan rate, gains, and other important scanning parameters automatically for a given sample. Not only does this process protect both fragile probes and samples, it significantly reduces the time required to obtain high resolution images. PF-QNM is compatible for AFM imaging in fluid; therefore, it has extensive application for imaging biologically relevant materials.

The method presented in this paper describes the application of PF-QNM to obtain images of a bacterial red-light photoreceptor, RpBphP3 (P3), from photosynthetic *R. palustris* in its light-adapted state. Using this method, individual protein dimers of P3 and aggregates of dimers have been observed on a mica surface in the presence of an imaging buffer. With appropriate adjustments to surface and/or solution concentration, this method may be generally applied to other biologically relevant macromolecules and soft materials.

Video Link

The video component of this article can be found at https://www.jove.com/video/52164/

Introduction

Atomic force microscopy (AFM) has become a very important tool for investigating the structural and mechanical properties of surfaces, thin films, and single molecules since its invention in 1986 (**Figure 1**).[1-3] Using a liquid-cell, the method has become particularly useful in studies of biological macromolecules and even living cells in a physiologically relevant environment.[4-10] Tapping-mode AFM has traditionally been used for imaging soft materials or loosely bound molecules to the surface, since contact-mode AFM is typically unsuitable due to the damage caused by the lateral forces exerted on the sample by the cantilever.[11] Tapping-mode AFM substantially reduces these forces by having the tip intermittently touch the surface rather than being in constant contact. In this mode, the cantilever is oscillated at or near its resonant frequency normal to the surface. Similarly to contact-mode AFM, topography is analyzed by plotting the movement of the z-piezo as a function of xy (distance).

The cantilever dynamics can be quite unstable at or near resonance; therefore, they are very challenging to automate outside of a “steady-state” situation. Specifically, these dynamics depend on both the sample properties and scanning environment. For a soft molecule adsorbed to a hard(er) surface, a well-tuned feedback loop for the molecule may lead to feedback oscillation for the surface. Operation in fluid further complicates the tuning of the cantilever. Changes in temperature or fluid levels require constant readjustment of set point, gains, and other imaging parameters. These adjustments tend to be very time-consuming and challenging for users.

Peak Force Quantitative Nanomechanical Property Mapping (PF-QNM), like tapping mode AFM, avoids lateral interactions by intermittently contacting the sample (**Figure 2**).[12-15] However, PF-QNM operates in non-resonant mode and frequencies much lower than tapping-mode AFM. This eliminates the tuning challenges of tapping-mode AFM, particularly those exacerbated by the presence of fluid. With PF-QNM, images are collected by taking a force response curve at every point of contact. With the addition of ScanAsyst software,[15] adjustment of the scanning parameters can be automated and a high-resolution image obtained in a matter of minutes by even inexperienced users. Once the user becomes more familiar with the AFM, any or all of the automated parameters may be disabled at any time which permits the experimentalist

to fine tune the image quality manually. Since its inception, PF-QNM has been applied to map bacteriorhodopsin, a membrane protein, and other native proteins at the submolecular level.[16-18] For bacteriorhodopsin, there is a direct correlation between protein flexibility and X-ray crystallographic structures.[12] PF-QNM has been utilized to investigate living cells with high resolution.[19,20] Furthermore, PF-QNM data has elucidated important connections between structure and mechanics within the erythrocyte membrane that are critical for cell integrity and function.[21]

We have employed scanning probe microscopy (SPM) methods,[22] including AFM,[23] to study the structure of red-light photoreceptors called bacteriophytochromes (BphPs).[24,25] They consist of a light sensing module covalently linked to a signaling-effector module such as histidine kinase (HK).[26] The light-sensing module typically contains a bilin chromophore which undergoes structural transformation upon absorption of a photon, with a series of structural changes reaching the signaling-effector module and leading to a global transformation of the entire protein.[24,27-29] Based on this transformation, there are two distinct light absorbing states of BphPs, a red and far-red light absorbing state, denoted as Pr and Pfr. Pr is thermally stable, dark-adapted state for most BphPs.[28] The molecular basis of Pr/Pfr photoconversion is not entirely understood due to limited structural knowledge of these proteins. With the exception of one structure from *D. radiodurans*,[30] all published X-ray crystallographic structures of these proteins are in the dark-adapted state and lack effector domain. The intact BphPs are too large to be effectively studied by Nuclear Magnetic Resonance (NMR) and are notoriously difficult to crystallize in their intact form (particularly in the light-adapted state) for X-ray crystallography. BphPs have recently been engineered as infrared fluorescent protein markers (IFP's).[31] Structural characterization of these proteins can further aid in effective IFP design.[32-36]

The focus of this article is to present a procedure for imaging of BphPs using liquid-cell AFM via PF-QNM. The method is demonstrated by studies of the light-adapted state of the bacteriophytochrome RpBphP3 (P3) from the photosynthetic bacterium *R. palustris*. The AFM procedure presented here is convenient and straightforward approach for imaging of proteins as well as other biological macromolecules. With this method, structural details of individual molecules can be collected in a short period of time, similar to an upper-level science course laboratory session. Through measuring cross-sections and completing further dimensional analyses, experimental data can be compared to useful computational models.[37-42]

Protocol

1. Computer and Microscope Set Up

1. Open the valve of the N_2 cylinder and adjust the knobs to ensure the air table is floating and level.
2. Turn on the computer, controller, and fiber optic light in this order.
3. Set the scanner to AFM/LFM mode and center the camera over the AFM head.
4. Open software. Select experiment category “Nanomechanical Properties”, “Quantitative Nanomechanical Mapping” under experiment group, and “PeakForce QNM in Fluid” under experiment. Click Load Experiment and then Setup.
5. Focus the camera using the Z objective to see the surface of the stage. Using the coarse up/down piezos move the stage approximately 1 mm below the surface of the AFM head aperture.

2. Preparation of Mica Surface

1. Press an adhesive sticker onto the face of a clean sample support disk (15 mm diameter, 0.8 mm thick). Push a mica V-4 grade disk (25 x 25 x 26 mm) onto the adhesive until firmly attached.
2. Rub a piece of clear tape onto the mica ensuring it is fully adhered with no air bubbles. Pull the tape off the mica from one side to evenly cleave it. Repeat if necessary to insure the mica is flat.
3. Grip the support disk, clean mica side up, with a pair of circular tweezers (disk grippers), and place onto the scanner. The mica should be below the level of the AFM head aperture.

3. Fluid Cell Assembly and Imaging of Mica Surface

1. Rinse the fluid cell, O-ring, syringe adapter, hose adapter, and the ejection hose in 100% ethanol. Rinse the fluid cell in DI water. Let all parts air dry completely.
2. Push the hose adapter into the port on the clean fluid cell. Gently press the O-ring into the center indentation of the fluid cell using flat headed tweezers.
3. Press the spring lightly on the probe retainer clip and turn it away from the groove for the tip.
4. Grasp the probe on the long end away from the tip with flat headed tweezers. Place the probe into the groove with the tip facing the center of the cell. Push the spring in and adjust the retainer clip over the probe to secure it (**Figure 1B**).
5. Check the clamp on the AFM to ensure it is fully retracted (**Figure 1C**).
6. Place the fluid cell, O-ring and probe facing downwards, on top of the mica sample. Allow the fluid cell to rest onto the studs of the AFM. Lower the clamp to stabilize the fluid cell on the stage. Press the down switch on the microscope until a visual inspection shows the O-ring firmly compressed between the support disk and the fluid cell.
7. While watching the monitor, focus the coarse adjustment knob to visualize the top of the fluid cell on the screen.
8. Move the microscope until there is a clear image of the tip using the X/Y adjustment knobs and the Z objective. The tip will appear like a metallic, golden triangle. Move the tip closer to the sample surface using the down piezo lever on the microscope. Focus on the reflection of the tip. Keep track of the actual cantilever in relationship to its reflection. At this stage, they should be closely aligned, but not completely overlapping.
9. Attach the syringe adapter to a sterile 1 ml syringe. Attach one end of the ejection hose to the syringe adapter and place the other end of the hose in the container of buffer solution. Fully extend the plunger of the syringe.

10. Attach the hose to the hose adapter on the fluid cell. Gently press the plunger until fluid fully fills the center chamber. Check the cell to insure there are no air bubbles. Check to see there is no fluid spilling out from the fluid cell onto the microscope. Place the syringe on a raised solid support.
11. Use the camera feed and the X/Y translation knobs to locate the laser on the screen (a diffuse red dot). Using the laser movement control knobs, move the laser onto the tip.
12. Finely adjust the laser and mirror controls until the sum signal displayed on the microscope is maximized (value = 4 - 6).
13. Adjust the angle of the quadrant diode using the knobs on the left rear side and the top left side of the scan head to lower the vertical and horizontal deflections displayed on the microscope as close to zero as possible (± 0.1).
14. In the software, select acquisition options. At a minimum, select height (trace and retrace), peak force error, and deformation. The other options are user dependent and can be tailored based on the specific information desired by the experimentalist.
15. Select “line” for RT Plane Fit in each acquisition window. Select “none” for the OT Plane Fit in the height windows. Set the X and Y offset and scan angle to zero, if not already done.
16. Set the scan rate to 1 Hz, the sample per line to 256, the ScanAsyst auto control to individual, and the ScanAsyst auto Z limit to off. Change the Z limit to 500 nm. Set scan size to 1 µm.
17. Click engage. At this point, the tip approaches the surface. While the tip is approaching, observe Z piezo voltage change in the lower left hand corner of the screen. If the tip goes outside of range, withdraw the tip and re-approach. If this is unsuccessful, the tip may need to be changed in order to have a successful approach. Once the tip is engaged, the lines will start to appear on each of the acquisition windows that will compose an image.
18. Take images of mica at 1 x 1 µm and zoom in slowly to ensure that the mica surface is clean and flat. Click continuous capture to save images as they appear. Zoom in and move around the surface as desired.

4. Protein Deposition and Preparation of Sample for Imaging

1. Obtain purified protein sample[38] and keep on ice. If stored in a freezer, thaw sample on ice for 5 min.
2. Dilute the protein to 0.0010 mg/ml using refrigerated imaging buffer solution. The imaging buffer used here is 15 mM Tris-HCl (pH = 8.0), 150 mM NaCl, and 15 mM $MgCl_2$.
3. Fill a 4 chamber (100 x 15 mm) Petri dish with refrigerated imaging buffer solution. Fill each chamber with at least 5 ml of solution. Gently mix the diluted protein solution with the tip attached to micropipettor.
4. Apply 200 µl of the diluted protein solution to the surface of mica already prepared. After 30 sec, pick up the protein/mica surface with the circular tweezers (disk grippers). Hold the sample parallel to the lab bench.
5. While holding the sample, immediately immerse the sample in the buffer solution contained in the first quadrant of the Petri dish (**step 4.2**) while ensuring that the sample is parallel to the basin of the Petri dish. After 1 sec, remove the sample.
6. Continuing to hold the sample parallel to the basin of the Petri dish, repeat **step 4.5** for the remaining three quadrants.
7. Place the disk on a dry dust free cloth to soak up excess moisture and transfer the disk onto the stage of the microscope. Do not touch the actual surface with the cloth. Do not allow the sample to dry.
8. Repeat **steps 3.6 - 3.16**.

5. Imaging Proteins on Mica

1. Click on check parameters box on the left hand side of the screen. Spring size and tip radius should be set based on the tip being used.
2. Click engage. Similarly to the mica imaging process (**step 3.17**), observe the z-piezo window as the tip approaches.
3. Allow the scanner to image the same area for at least two consecutive passes. Click continuous capture to save each image collected.
4. Move the scanner to a new region and/or change the image size as desired.
5. After the automated software has finished adjusting the scanning parameters for a particular image size, turn the software off.
6. Manually adjust scan rate, z limit, the number of lines, and voltage in order to fine tune the focus of the image. If the image becomes too far out of focus, turn software back on to return the original starting position. To increase the resolution of an image while zooming in on a protein, decrease the scan rate and increase the number of lines proportionally.
7. After the experiment, clean the liquid-cell with 100% ethanol and rinse with DI H_2O. Allow the liquid cell to fully dry.
8. Open the data software to process raw data images. First, flatten the image by clicking on the flatten icon. Select $Zero^{th}$ order and click execute. Depending on the image, a plane fit may be necessary to obtain an appropriately flat image. In this case, select the plane fit icon and draw a plane of a flat area of the image using the cursor. Click execute. Repeat as necessary
9. Select the cross-section tab to measure the dimensions of the protein. Draw a line with the cursor move it over the molecule or area to be analyzed. Repeat for multiple areas and the software will generate an overlay. Export the picture or the data used to generate picture in a format compatible to other software and drawing programs.

Representative Results

Representative AFM images of a photoreceptor protein, P3, in its light-adapted state are presented in **Figures 3** and **4**. A freshly-cleaved mica substrate (**Figure 3A**) is a suitable, flat surface for protein adsorption. Collecting an image of clean mica as a negative control is important for several reasons. First, it insures the liquid cell is clean and no residual materials from previous experiments will contaminate the surface. Second, it tests the quality of the probe. If the probe is dirty or deformed, this will appear in the image as streaks or present itself as noise. Finally, a clean mica image confirms the probe can be appropriately tuned for future experiments.

Single photoreceptor protein dimers can be observed using PeakForce QNM if the surface coverage is appropriate (**Figure 3B,C**). Arrows signal individual dimers; the asterisk denotes a protein aggregate. The concentration of the protein sample, deposition time, and the ionic strength of the imaging buffer impact the surface coverage.[23] For a high distribution of single molecules, very dilute solutions with short deposition times are

required. For example, doubling the deposition time yields a high distribution of even larger aggregates. If the protein concentration is increased to 0.100 mg/ml, a thin film of photoreceptors is observed without modifying the deposition time or buffer ionic strength.

Using image analysis software, the cross-sections of the proteins may be measured after the image is flattened (**Figure 4**). The cross-sections provide xy-data with corresponding height measurements. These measurements can be used to provide structural details, protein/surface interactions, mechanical strength, etc. The xy-data may be convoluted by the AFM probe; however, this effect can be minimized by using a sharper probe. In fact, the choice of probe is a delicate balance between an acceptable amount of convolution and the resistance of the imaged material to damage by a sharp probe. Tip convolution may also be subtracted from the image, if necessary, by using appropriate software.

These pictures may be directly compared to previously published images collected using tapping-mode AFM.[20] The measured dimensions of P3 on mica using PeakForce QNM are within 5% of values obtained with tapping-mode AFM.

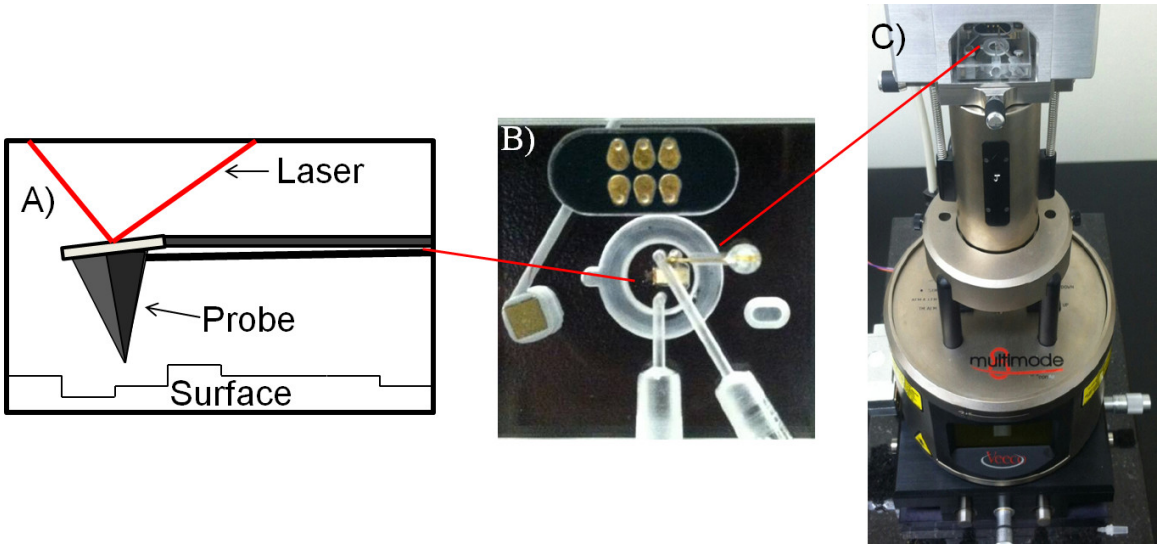

Figure 1. Liquid-Cell Atomic Force Microscopy. (A) Laser, cantilever, probe, and surface alignment. The probe and cantilever are affixed inside the liquid cell. **(B)** Liquid cell. The probe, cantilever, and sample are completely immersed in the fluid. **(C)** Complete assembly. The liquid cell is attached to a micrometer. The picture shows the optical head and scanner in relationship to the liquid cell. Please click here to view a larger version of this figure.

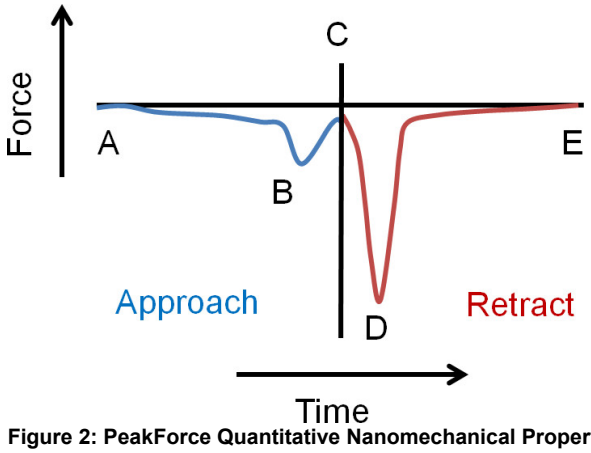

Figure 2: PeakForce Quantitative Nanomechanical Property Mapping. This is an illustration for a small peak force. **(A)** Approach **(B)** Jump to contact **(C)** Peak Force **(D)** Adhesion **(E)** Retract. The figure was reproduced and adapted with permission.[15]

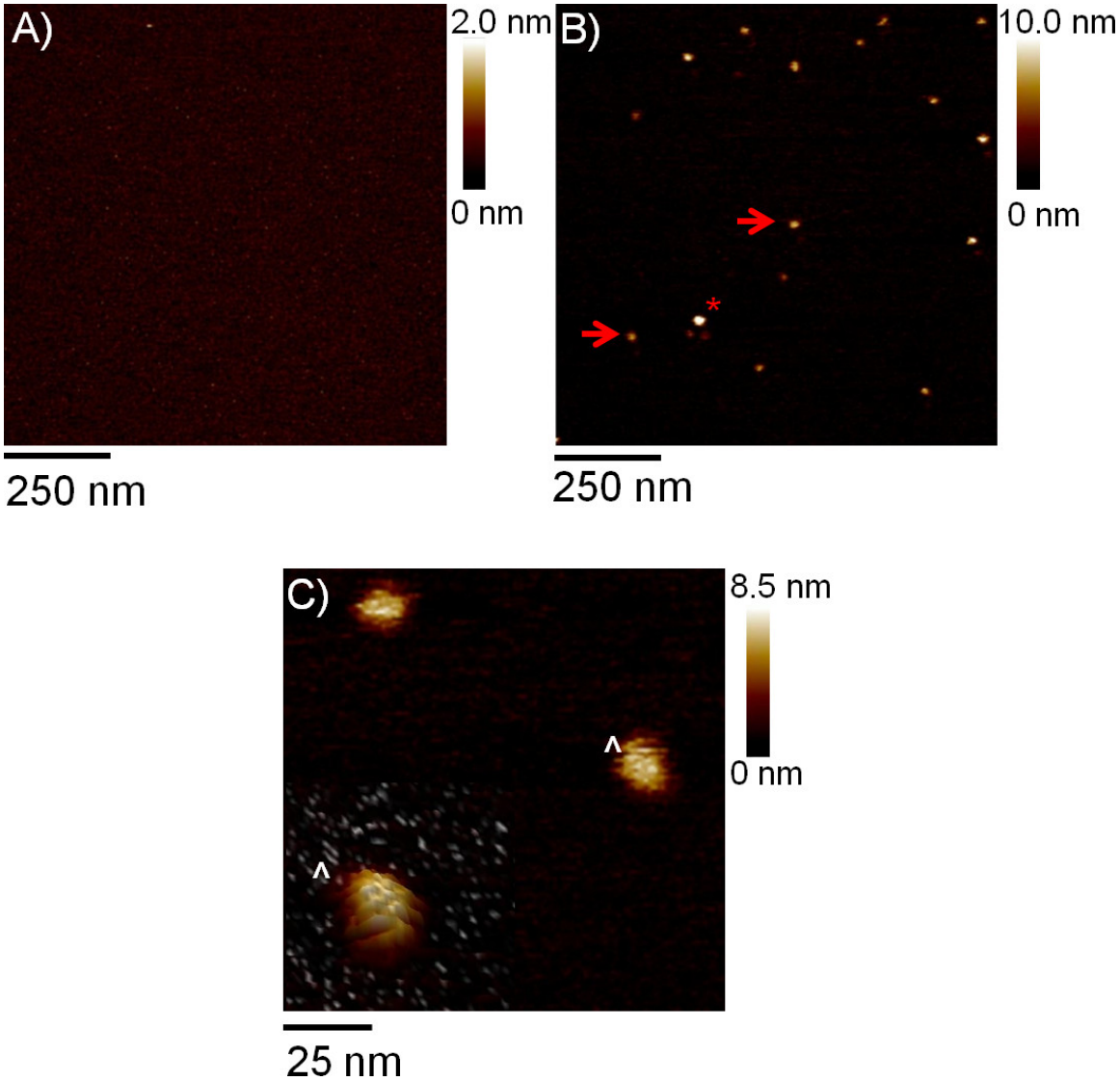

Figure 3. Atomic Force Microscopy of P3 on Mica. (A) Image of clean mica (1 x 1 µm). **(B)** Image (1 µm x 1 µm) of P3 applied to mica. The arrows indicate examples of single protein dimers. The asterisk denotes an aggregate of protein dimers. **(C)** Image (170 x 170 nm) of two protein dimers with a three-dimensional inset of a single dimer. The caret designates which protein dimer is present in the inset. All images were taken in the presence of the imaging buffer (protein concentration = 0.0010 mg/ml for deposition). Please click here to view a larger version of this figure.

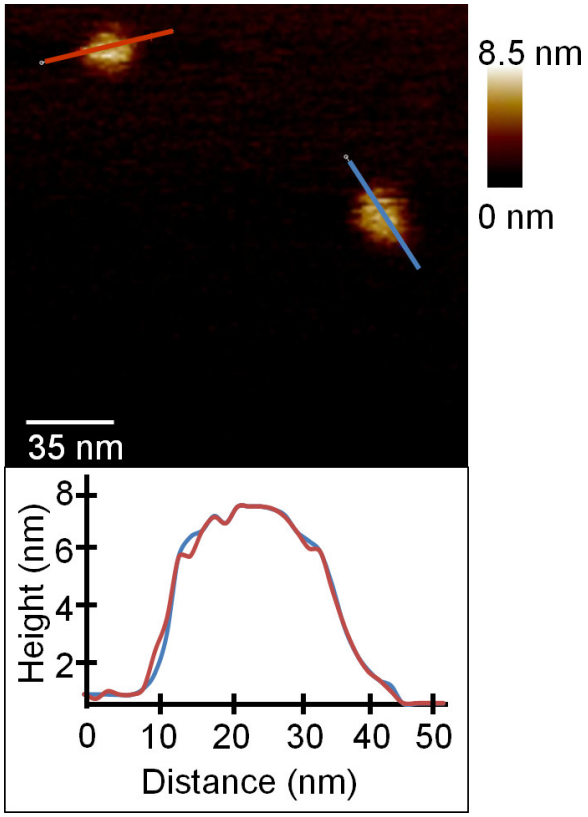

Figure 4. Cross-Sectional Analysis of P3 on Mica. AFM image of P3 on mica (170 x 170 nm) with cross-sectional height/distance measurements noted for two dimers. Please click here to view a larger version of this figure.

Discussion

AFM is a scanning probe microscopy method fully capable of imaging proteins and other biological macromolecules in physiologically relevant conditions. In comparison to X-ray crystallography and NMR, one limitation of AFM is its inability to achieve the same resolution, particularly lateral resolution. When using AFM to analyze a molecule on any surface, the impact of the surface and the probe on the image of the molecule must also be considered when data are analyzed. Deconvoluting of the probe's impact on the acquired image may be completed with appropriate software. Developing theoretical models to compare to experimental outcome can also prove to be quite useful.

In this paper, AFM images of a bacterial red-light photoreceptor, RpBphP3 (P3), are presented (**Figure 3**). While the descriptions of the microscope assembly and the software operation are specific to the particular instrument model employed, the mica and protein sample preparation procedures are general and may be applied to any AFM experiment.

A few critical steps of this protocol must be followed in order to obtain the desired protein coverage on the mica surface. First, the diluted protein solution must be gently mixed before it is applied to the mica surface (**step 4.3**). Due to the high molecular weight of P3, the depositing solution is quite colloidal; therefore, P3 settles to the bottom of the tube over time making the solution non-homogeneous. A gentle stir remedies this issue. Second, once the protein is applied, the surface must be rinsed to remove any loosely bound molecules (**step 4.5 - 4.6**). If loosely bound P3 remains on the surface, the molecules will be either released into the solution when the liquid cell is filled with buffer solution and/or picked up by the AFM probe during the experiment. Both of these events hinder a successful imaging experiment. If the liquid-cell becomes contaminated with P3, it must be disassembled and thoroughly cleaned. If the AFM probe picks up a molecule, it typically must be replaced or image quality is sacrificed. Finally, the method of rinsing the protein sample is critical to obtaining excellent images. Mica is a non-selective surface to P3; therefore, the molecules should be found to be oriented randomly. The method of rinsing described in the protocol is one way to avoid rearranging the molecules on the surface into one single orientation. The key is to always keep the sample wet and to avoid holding the surface at angle and literally spraying the surface with buffer. If the sample is rinsed by dipping, while holding it parallel to the basin of a Petri dish, the distortion of P3 on the surface by force currents of the buffer solution is minimized.

All of the parts to the liquid cell, probe, scanner, and optical head are very delicate and must be handled with care. The springs that hold the scanner and optical head together are very strong. It is imperative to keep a hand on the scanner when assembling or dissembling any of the pieces. For PF-QNM with ScanAsyst software, as described in the protocol, it is essential to turn off the automated software control of the Z-limit and set this value to at least 500 nm if the original scan size is 1 µm (**step 3.16**). This protects the scanner if the surface has become unexpectedly rough or has become contaminated. Once a single image has been collected and it is confirmed that the imaged area is smooth, the Z-limit may be adjusted downward manually to achieve higher resolution images. It is crucial to readjust the Z-limit back to at least 500 nm when the scanner is moved to a new area of the surface or if the tip is retracted for any reason.

While this paper has been focused on using PF-QNM to obtain high-quality topographical images, the method itself can provide a library of additional information about the mechanical strength and flexibility of surface structures. This feature can lead to further insights about

functionality by simply selecting the appropriate channels during the experiment.[16,18] With appropriate changes to the concentration of the depositing solution and/or the surface, this method can be general for using PF-QNM to investigate biological macromolecules by liquid-cell AFM. With the automated help of software, students in upper-level science courses with no prior experience with AFM can complete a liquid-cell AFM experiment much more quickly than with the traditional tapping-mode AFM. Students can experience the basics of AFM and get a taste of the interdisciplinary research made possible by this powerful technique within a typical 3 - 4 hr laboratory section time constraint.

Disclosures

There are no competing financial interests or conflicts of interest.

Acknowledgements

The NSF-MRI program (CHE: 1229103) is acknowledged for funding the purchase of new control electronics, software, liquid cells, and other equipment needed to assemble a dual AFM/STM. We acknowledge the shared facilities at The University of Chicago NSF-MRSEC program (DMR-0820054) for assistance with AFM instrumentation, training, and imaging, and for instrument time made available by the Materials Research Facilities Network (DMR-0820054). We particularly thank Dr. Qiti Guo, Dr. Justin Jureller, and Prof. Ka Yee Lee for welcoming our students before the funding of the NSF-MRI proposal that brought the necessary instrumentation to our campus. We acknowledge funding from a Title III STEM grant (ID: P031C110157) awarded to Northeastern Illinois University that provided summer research stipends for students and faculty as well as support for consumable supplies. Finally, we acknowledge Bruker-Nano, Inc. for continued instrumental support and for permission to reproduce a plot showing the mechanism of PeakForce QNM and to use the word ScanAsyst to describe the automated software.

References

1. Binnig, G., Quate, C. F., & Gerber, C. Atomic Force Microscope. *Phys. Rev. Lett.* **56**, 930-933, DOI: http://dx.doi.org/10.1103/PhysRevLett.56.930 (1986).
2. Sonnenfeld, R., & Hansma, P. K. Atomic-Resolution Microscopy in Water *Science.* **232**, 211-213, DOI:10.1126/science.232.4747.211 (1986).
3. Nikiforov, M. P., & Darling, S. B. Concurrent Quantitative Conductivity and Mechanical Properties Measurements of Organic Photovoltaic Materials using AFM. *J. Vis. Exp.* **71**, doi:10.3791/50293 (2013).
4. Bahatyrova, S. *et al.* The Native Architechure of a Photosynthetic Membrane. *Nature.* **430**, 1058-1061, doi:10.1038/nature02823 (2004).
5. Sturgis, J. N., Tucker, J. D., Olsen, J. D., Hunter, C. N., & Niederman, R. A. Atomic Force Microscopy Studies of Native Photosynthetic Membranes. *Biochem.* **48**, 3679-3698, doi:10.1021/bi900045x (2009).
6. Pelling, A. E., Li, Y., Shi, W., & Gimzewski, J. K. Nanoscale visualization and characterization of *Myxococcus xanthus* cells with atomic force microscopy. *Proc. Natl. Acad. Sci. U S A.* **102**, 6484-6489, doi: 10.1073/pnas.0501207102 (2005).
7. Viani, M. B. *et al.* Probing Protein-Protein Interactions in Real-Time. *Nature: Structural Biology.* **7**, 644-648, doi:10.1038/77936 (2000).
8. Hook, F., Kasemo, B., Grunze, M., & Zauscher, S. Quantitative Biological Surface Science, Challenges and Recent Advances. *ACS Nano.* **2**, 2428-2436, **DOI:** 10.1021/nn800800v (2008).
9. Thomas, G., Burnham, N. A., Camesano, T. A., & Wen, Q. Measuring the Mechanical Properties of Living Cells Using Atomic Force Microscopy. *J. Vis. Exp.* **76**, doi:10.3791/50497 (2013).
10. Murphy, P. J. M., Shannon, M., & Goertz, J. Visualization of Recombinant DNA and Protein Complexes Using Atomic Force Microscopy. *J. Vis. Exp.* **53**, doi:10.3791/3061 (2011).
11. Poggi, M. A. *et al.* Scanning Probe Microscopy. *Anal. Chem.* **76**, 3429-3444, **DOI:** 10.1021/ac0400818 (2004).
12. Rico, F., Su, C., & Scheuring, S. Mechanical Mapping of Single Membrane Proteins at Submolecular Resolution. *Nano Letters.* **11**, 3983-3986, doi: 10.1021/nl202351t (2012).
13. Foster, B. The State of Microscopy for 2012. *Amer. Lab.* **43**, 4-6 (2011).
14. Guzman, H. V., Perrino, A. P., & Garcia, R. Peak Forces in High-Resolution Imaging of Soft Matter in Liquid. *ACS Nano.* **7**, 3198-3204, doi: 10.1021/nn4012835 (2013).
15. Kaemmer, S. B. Introduction to Bruker's ScanAsyst and PeakForce Tapping AFM Technology. *Bruker Nano Surfaces Division.* (2011).
16. Dufrêne, Y. F., Martinez-Martin, D., Medalsy, I., Alsteens, D., & Muller, D. J. Multiparametric imaging of biological systems by force-distance curve-based AFM. *Nature Methods.* **10**, 847-854, doi:10.1038/NMETH.2602 (2013).
17. Pfreundschuh, M., Martinez-Martin, D., Mulvihill, E., Wegmann, S., & Muller, D. J. Multiparametric high-resolution imaging of native proteins by force-distance curve–based AFM. *Nature Protocols.* **9**, 1113-1130, doi:10.1038/nprot.2014.070 (2014).
18. Pfreundschuh, M., Alsteens, D., Hilbert, M., Steinmetz, M. O., & Muller, D. J. Localizing Chemical Groups while Imaging Single Native Proteins by High-Resolution Atomic Force Microscopy. *Nano Letters.* **14**, 2957-2964, doi:dx.doi.org/10.1021/nl5012905 (2014).
19. Berquanda, A. *et al.* Atomic Force Microscopy Imaging of Living Cells. *Microscopy Today* 18, 8-14 (2010).
20. Heua, C., Berquand, A., Elie-Cailleb, C., & Nicoda, L. Glyphosate-induced Stiffening of HaCaT Keratinocytes, a Peak Force Tapping Study on Living Cells. *J. Struc. Biol.* **178**, 1-7, doi: 10.1016/j.jsb.2012.02.007 (2012).
21. Picas, L., Rico, F., Deforet, M., & Scheuring, S. Structural and Mechanical Heterogeneity of the Erythrocyte Membrane Reveals Hallmarks of Membrane Stability. *ACS Nano.* **7**, 1054-1063, doi: 10.1021/nn303824j (2013).
22. Tobias, F. G. *et al.* Scanning Probe Microscopy of Bacterial Red-Light Photoreceptors. *Mater. Res. Soc. Symp. Proc.* **1465**, doi:10.1557/opl.2012.1006 (2012).
23. Sorenson, B. A. *et al.* Domain Structure of a Unique Bacterial Red Light Photoreceptor as Revealed by Atomic Force Microscopy. *Mater. Res. Soc. Symp. Proc.* **1652**, doi:10.1557/opl.201.259 (2013).
24. Rockwell, N. C., & Lagarias, J. C. The structure of phytochrome: a picture is worth a thousand spectra. *Plant Cell.* **18**, 4-14, doi:10.1105/tpc.105.038513 (2006).
25. Rockwell, N. C., Shang, L., Martin, S. S., & Lagarias, J. C. Distinct classes of red/far-red photochemistry within the phytochrome superfamily. *Proc. Natl. Acad. Sci. USA.* **106**, 6123-6127, doi: 10.1073/pnas.0902370106 (2009).

26. Noack, S., Michael, N., Rosen, R., & Lamparter, T. Protein conformational changes of Agrobacterium phytochrome Agp1 during chromophore assembly and photoconversion. *Biochem.* **46**, 4164-4176, **DOI:** 10.1021/bi602419x (2007).
27. Noack, S., & Lamparter, T. Light modulation of histidine-kinase activity in bacterial phytochromes monitored by size exclusion chromatography, crosslinking, and limited proteolysis. *Methods of Enzymology.* **423**, 203-221, DOI: 10.1016/S0076-6879(07)23009-5 (2007).
28. Rockwell, N. C., Su, Y. S., & Lagarias, J. C. Phytochrome structure and signaling mechanisms. *Annual Review Plant Biology.* **57**, 837-856, DOI: 10.1146/annurev.arplant.56.032604.144208 (2006).
29. Bhoo, S. H., Davis, S. J., Walker, J., Karniol, B., & Vierstra, R. D. Bacteriophytochromes Are Photochromic Histidine Kinases Using a Biliverdin Chromophore. *Nature.* **414**, 776-779, doi:10.1038/414776a (2001).
30. Takala, H. *et al.* Signal amplification and transduction in phytochrome photosensors. *Nature.* **509**, 245-248, doi:10.1038/nature13310 (2014).
31. Filonov, G. S. *et al.* Bright and Stable Near-Infared Fluorescent Protein for *in vivo* Imaging. *Nature Biotech.* **29**, 757-761, doi:10.1038/nbt.1918 (2011).
32. Samma, A. A., Johnson, C. K., Song, S., Alvarez, S., & Zimmer, M. On the Origin of Fluorescence in Bacteriophytochrome Infrared Fluorescent Proteins. *J. Phys. Chem. B.* **114**, 15362-15369, doi: 10.1021/jp107119q (2011).
33. Lehtivuori, H. *et al.* Fluorescence Properties of the Chromophore-Binding Domain of Bacteriophytochrome from *Deinococcus radiodurans*. *J. Phys. Chem. B.* **117**, 11049-11057, doi: 10.1021/jp312061b (2013).
34. Toh, K. C. *et al.* Primary Reactions of Bacteriophytochrome Observed with Ultrafast Mid-Infrared Spectroscopy. *J. Phys. Chem. A.* **115**, 3778-3786, doi: 10.1021/jp106891x (2011).
35. Auldridge, M. E., Satyshur, K. A., Anstrom, D. M., & Forest, K. T. Structure-guided engineering enhances a phytochrome-based infrared fluorescent protein. *J. Biol. Chem.* **287**, 7000-7009, doi: 10.1074/jbc.M111.295121 (2012).
36. Toh, K. C., Stojkovic, E. A., van Stokkum, I. H., Moffat, K., & Kennis, J. T. Proton-transfer and hydrogen-bond interactions determine fluorescence quantum yield and photochemical efficiency of bacteriophytochrome. *Proc. Natl. Acad. Sci. U S A.* **107**, 9170-9175, doi:10.1073/pnas.0911535107 (2010).
37. Yang, X., Stojkovic, E. A., Kuk, J., & Moffat, K. Crystal structure of the chromophore binding domain of an unusual bacteriophytochrome, RpBphP3, reveals residues that modulate photoconversion. *Proc. Natl. Acad. Sci. USA.* **104**, 12571-12576, doi:10.1073/pnas.0701737104 (2007).
38. Yang, X., Kuk, J., & Moffat, K. Crystal structure of *Pseudomonas aeruginosa* bacteriophytochrome: photoconversion and signal transduction. *Proc. Natl. Acad. Sci. USA.* **105**, 14715-14720, doi:10.1073/pnas.0806718105 (2008).
39. Woitowich, N. K., Garrido, C., Ozarowski, W., & Stojkovic, E. A. Preliminary X-ray Crystallographic and Structural Analyses of a Bacteriophytochrome from *Stigmatella aurantiaca*. *The FASEB Journal.* **25**, 928.15 (2011).
40. Wagner, J. R., Zhang, J., Brunzelle, J. S., Vierstra, R. D., & Forest, K. T. High resolution structure of Deinococcus bacteriophytochrome yields new insights into phytochrome architecture and evolution. *J. Biol. Chem.* **282**, 12298-12309, doi:10.1074/jbc.M611824200 (2007).
41. Wagner, J. R. *et al.* Mutational analysis of *Deinococcus radiodurans* bacteriophytochrome reveals key amino acids necessary for the photochromicity and proton exchange cycle of phytochromes. *J. Biol. Chem.* **283**, 12212-12226, doi:10.1074/jbc.M709355200 (2008).

